

If the  $\phi$  of eq 18 is identified with the quantity  $(\phi_s - \phi_u)$ , then from eq 6, 7, and 18 the formula for the effective dielectric constant is

$$D_E = \left[ 1 + 2(1 - D) \left( \frac{b}{a} \right) S_1 \right]^{-1} \quad (19)$$

The effective dielectric constant is plotted in Figure 3.  $D_E$  is plotted for the ratio  $b/a$  for  $D = 2.0$  (curve I) and  $D = 5.0$  (curve II). In the case where  $b = 3.0 \text{ \AA}$  and  $a = 3.61$ ,  $D_E$  is 0.729 for  $D = 5.0$ .<sup>20</sup>

For a dipole substituent of finite length  $l$  with charges  $+q$  and  $-q$  at the end points  $a_1$  and  $a_2$  on the  $z$  axis, the potential at the proton, also on the  $z$  axis is

$$\phi = qf_1 - qf_2 = p(f_1 - f_2)/l \quad (20)$$

$$p = ql$$

where  $p$  is the dipole moment of the charge distribution. If  $q$  is increased and at the same time  $l$  goes to zero in such a manner that the product  $p$  remains constant, there is obtained for the potential due to the point dipole

$$\phi = p \lim_{l \rightarrow 0} (f_1 - f_2)/l = p \nabla f \quad (21)$$

(20) The most arbitrary quantity leading to the above results is the radius of the sphere. If the size of the sphere is varied but its weight is held constant,  $D$  will vary. However, under such circumstances the ratio  $b/a$  also varies, but in such a manner that  $D_E$  remains relatively constant. Thus, the value of  $D_E$  is not extremely dependent on the size of the sphere chosen. For example, in the case of the potential due to the point charge, when the radius of the sphere is 2.8,  $b/a = 0.7756$ ,  $D = 7.0934$ , and  $D_E = 0.725$ . When the radius of the sphere is 3.5,  $b/a = 0.9695$ ,  $D = 2.597$ , and  $D_E = 0.771$ .

where the derivative  $\nabla f$  is to be evaluated at the location of the point dipole.

In the special case where the point  $r, \theta$  and the dipole are equidistant from the center of the sphere and colinear with it and the direction of the dipole is toward the center of the sphere, from eq 17 and 21

$$\phi = \frac{p}{(2a)^2} \left\{ 1 + 4(1 - D) \frac{b}{a} \sum_{n=0}^{\infty} \frac{n(n+1)}{nD + n + 1} \left( \frac{b}{a} \right)^{2n} \times (-1)^n \right\} \quad (22)$$

If the potential  $\phi$  of eq 22 is now identified with  $(\phi_s - \phi_u)$ , then in this case  $D_E$  becomes, from (6), (8), and (22)

$$D_E = \left[ 1 + 4(1 - D) \frac{b}{a} S_2 \right]^{-1} \quad (23)$$

$$S_2 = \sum_{n=0}^{\infty} \frac{n(n+1)}{nD + n + 1} \left( \frac{b}{a} \right)^{2n} (-1)^n$$

since  $\cos \alpha$  is 1.

In this paper the substituent is treated as a point dipole so that the above expression for an effective dielectric constant may be used. Curves III and IV of Figure 3 then give  $D_E$  for the ratio  $b/a$  for the two values of  $D$  of 2.0 and 5.0, respectively. For the case  $a = 3.6$  and  $b = 3.0$ ,  $D_E$  is 0.463 for  $D = 5.0$ .<sup>20</sup> The sums  $S_1$  and  $S_2$  were evaluated by a direct summation of terms and are accurate to at least eight decimal places after 100 terms.

## Infrared Spectra and Molecular Orbital Model for Carbon Monoxide Adsorbed on Metals

G. Blyholder and Marvin C. Allen

Contribution from the Department of Chemistry, University of Arkansas, Fayetteville, Arkansas 72701. Received September 9, 1968

**Abstract:** Infrared spectra are presented in the CO stretching region for CO adsorbed on V, Cr, Mn, and Co. Band maxima for the two main bands of each metal are located at V, 1940 and 1890  $\text{cm}^{-1}$ ; Cr, 1940 and 1880  $\text{cm}^{-1}$  (sh); Mn, 1950 and 1890  $\text{cm}^{-1}$ ; and Co, 2000 and 1880  $\text{cm}^{-1}$ . These data together with previously presented data for Fe, Ni, and Cu allow comparisons across the first transition series from V to Cu. A molecular orbital model for the  $\pi$ -electron system of CO adsorbed on a cluster of metal atoms successfully accounts for the shifts in position of the two principal bands as the metal is varied across the series.

The structures of species adsorbed on metal surfaces have been partially determined in a number of cases by using infrared spectroscopy. These studies have usually considered only one metal at a time, with each metal being treated as an isolated case. In the case of CO, which is one of the most studied adsorbates in infrared work, C-O stretching frequencies have been reported over a considerable spectral range, about 300  $\text{cm}^{-1}$ . While a few authors have discussed possible relationships between infrared band positions and the structure of chemisorbed CO, no previous attempts have been made to explain variations in band position from

one metal to another based on the electronic properties of the metal.

It was first suggested that infrared bands above 2000  $\text{cm}^{-1}$  represented a linear M-C-O structure, while bands somewhat below 2000  $\text{cm}^{-1}$  were due to a bridging CO group in which the carbon atom was bonded to two metal atoms.<sup>1</sup> Kavtaradze and coworkers have surveyed many metal carbonyl complexes, but no substituted metal carbonyls, and concluded that for chemisorbed CO bands in the 2000-2200- $\text{cm}^{-1}$  region

(1) R. P. Eischens, S. A. Francis, and W. A. Pliskin, *J. Phys. Chem.*, 60, 194 (1956).

reflect a linear structure while bands in the 1820–1880- $\text{cm}^{-1}$  region are due to bridge species.<sup>2</sup> In a novel approach Gardner and Petrucci<sup>3,4</sup> have selected some bands for correlation as “intermedions” which have electronic structures on a given metal differing by a whole number of electrons. Bands interspersed between their “intermedion” bands are referred to as carbonyls and are not considered. We prefer treating all of the bands equivalently on the basis of a single molecular orbital model.

Because the two main infrared bands for chemisorbed CO on a given metal vary in intensity independently of each other and cooling does not sharpen the very broad bands for chemisorbed CO,<sup>5</sup> we regard the surface as a collection of a large number of different sites which fall approximately into two groups. We have previously suggested<sup>6</sup> that for a variety of reasons it is not necessary to hypothesize the existence of a bridge structure to explain the infrared bands below 2000  $\text{cm}^{-1}$  and that these bands may be due to a linear M–C–O structure where CO is adsorbed on special sites such as edges, corners, and dislocations (referred to in the rest of this paper simply as corner sites), while bands near or above 2000  $\text{cm}^{-1}$  are due to a linear structure located in the middle of a lattice plane (referred to as middle sites). In this paper the success of this view as a model for molecular orbital calculations is demonstrated. The ability of a model of a bridge-bonded adsorbed CO species to fit the experimental data has not been examined.

In this paper we are concerned with the first transition metal series. Infrared spectral data for CO chemisorbed on Fe, Ni, and Cu have been reported numerous times.<sup>7,8</sup> In the case of Co, spectra for weakly held CO<sup>4</sup> and CO adsorbed after addition of other gases<sup>9</sup> have been reported, but these are not adequate for our purposes. In this paper new spectral data for CO adsorbed on V, Cr, Mn, and Co are presented. This allows direct comparison of data for the first transition metal series from V to Cu. By dealing with this series of metals it is expected that those factors which are important in determining the nature of the adsorption bond and vary in a consistent manner along this series will emerge.

Once having the data, the question of choosing a framework within which to handle the data arises. Full quantum-mechanical treatments of metallic crystal surfaces are particularly difficult because the presence of metallic character almost forces the inclusion of all atoms in the crystal. However, some limited progress has been made,<sup>10,11</sup> though unfortunately this progress does not yet include much about real transition metal crystals. Although various basis functions and mathematical techniques have been used, the qualitative

conclusions appear to be largely unaffected by the particular method. The most important conclusion from these approximate molecular orbital treatments is the appearance of localized electron states at the chemisorption bond if the electron-attracting power of the adsorbed atom is sufficiently different from that of the adsorbent atoms.

Recently it has been shown<sup>12</sup> that small finite models of one- and two-dimensional crystals (six-atom length or side) predict the same localized states as semiinfinite models and that an SCF–LCAO–MO calculation, using Roothaan's equations,<sup>13</sup> for a six-atom linear chain where each atom has one “s”-type valence electron indicates that simple Hückel models give a reasonably good description of the orbital changes that occur as the electron-attracting power of the end atom is changed to simulate chemical adsorption. Further it was shown that all orbitals, and not just localized states, must be used in calculating adsorption energies if correct relative energies for adsorption at different surface sites are to be obtained.

In one attempt to deal with transition metals, Bond<sup>14</sup> has considered qualitatively (no calculations) the overlap of olefin and CO orbitals with “d” orbitals of (100), (110), and (111) faces of face-centered cubic crystals. From this laboratory has come a molecular orbital model which has successfully dealt in a qualitative way with the adsorption of CO on a single metal.<sup>6</sup> In particular, the appearance of several C–O stretching bands on one metal, shifts in band position with adsorption of other gases, and the effect of alloying with another metal have been rationalized. In this paper the ability of a relatively simple molecular orbital calculation simulating the  $\pi$ -electron system for CO adsorbed on a cluster of metal atoms to render understandable the infrared data for CO adsorbed on the first transition metal series will be examined.

### Experimental System and Results

The experimental technique, which has been described in detail elsewhere,<sup>15</sup> consists of evaporating metal from an electrically heated tungsten filament in the presence of a small pressure of helium. The metal particles formed in the gas-phase deposit in a hydrocarbon oil matrix on the salt windows of an infrared cell. The gas to be studied is then admitted to the cell, and the spectrum of the chemisorbed species obtained. Spectra are recorded before and after admission of the gas to the cell. Five minutes of pumping has been found sufficient to remove all spectra due to gas-phase molecules.

The spectra were obtained using either a Perkin-Elmer Model 21 or a Model 337 spectrophotometer. The CO was passed through an activated charcoal trap cooled with liquid air.

The experimental results are shown in Figure 1. All of these spectra were recorded in this laboratory by the method described above except for CO on Cu. The Cu spectrum is a rough redrawing of that obtained by Eischens, Pliskin, and Francis.<sup>16</sup> Except for Cu, which

(2) N. N. Kavtaradze and N. P. Sokolova, *Zh. Fiz. Khim.*, **40**, 2957 (1966).

(3) R. A. Gardner and R. H. Petrucci, *J. Phys. Chem.*, **67**, 1376 (1963).

(4) R. A. Gardner and R. H. Petrucci, *J. Am. Chem. Soc.*, **82**, 5051 (1960).

(5) L. Lynds, *Spectrochim. Acta*, **20**, 1369 (1964).

(6) G. Blyholder, *J. Phys. Chem.*, **68**, 2772 (1964).

(7) L. H. Little, “Infrared Spectra of Adsorbed Species,” Academic Press, New York, N. Y., 1966.

(8) M. L. Hair, “Infrared Spectroscopy in Surface Chemistry,” Marcel Dekker, Inc., New York, N. Y., 1967.

(9) G. Blyholder and W. V. Wyatt, *J. Phys. Chem.*, **70**, 1745 (1966).

(10) J. Koutecky, *Advan. Chem. Phys.*, **9**, 85 (1965).

(11) T. B. Grimley, *Advan. Catalysis*, **12**, 1 (1960).

(12) G. Blyholder and C. A. Coulson, *Trans. Faraday Soc.*, **63**, 1782 (1967).

(13) C. C. J. Roothaan, *Rev. Mod. Phys.*, **23**, 69 (1951).

(14) G. C. Bond, *Discussions Faraday Soc.*, **41**, 200 (1966).

(15) G. Blyholder, *J. Chem. Phys.*, **36**, 2036 (1962).

(16) R. P. Eischens, W. A. Pliskin, and S. A. Francis, *ibid.*, **22**, 1786 (1954).

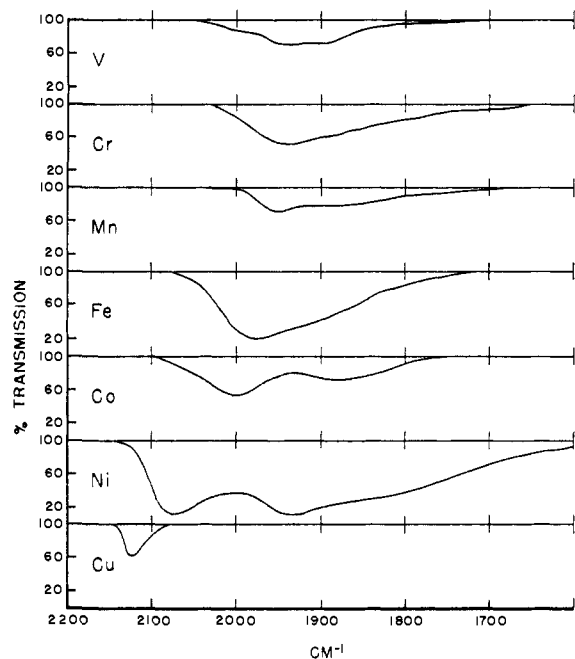


Figure 1. Infrared spectra of CO adsorbed on metals.

does not strongly chemisorb CO, the infrared bands are all very broad. The band maxima for the two main bands of each metal are located as shown in Table I.

Table I. Infrared Band Positions for Chemisorbed CO

| Metal | First band, $\text{cm}^{-1}$ | Second band, $\text{cm}^{-1}$ |
|-------|------------------------------|-------------------------------|
| V     | 1940                         | 1890                          |
| Cr    | 1940                         | 1880 (sh)                     |
| Mn    | 1950                         | 1890                          |
| Fe    | 1980                         | 1900 (sh)                     |
| Co    | 2000                         | 1880                          |
| Ni    | 2075                         | 1935                          |
| Cu    | 2120                         |                               |

### Molecular Orbital Models

The data will be considered first using the previously presented molecular orbital view of chemisorbed CO.<sup>6</sup> In this model a metal d, a carbon p, and an oxygen p orbital are considered to form a  $\pi$ -electron system. Of the three molecular orbitals resulting from this arrangement, the lowest in energy is bonding for both the carbon-metal and carbon-oxygen bonds and will be filled. The highest energy orbital is antibonding for both bonds and will be empty. The middle energy orbital, which is bonding for the carbon-metal bond and antibonding for the carbon-oxygen bond, will be partially filled. The extent of filling of this orbital will depend upon the competition between this orbital and orbitals on surrounding metal atoms for charge. Since this orbital is antibonding for the carbon-oxygen bond, increasing the charge in it will decrease the carbon-oxygen bond strength. Assuming a correlation between bond strength and infrared frequency, the C-O stretching frequency is expected to increase as charge is removed from this orbital.

As the atomic number increases in the first transition metal series from V to Cu, the energy level for the d orbitals decreases. This is readily seen in the valence-

state ionization potentials (VSIP), which for removal of a d electron from a  $3d^x4s^1$  state are V, 51,400; Cr, 57,900; Mn, 64,100; Fe, 70,000; Co, 75,000; Ni, 80,900; and Cu, 86,000  $\text{cm}^{-1}$ .<sup>17</sup> As the energy level of the metal decreases in this series, the competition between metal orbitals and the middle energy metal-carbon-oxygen molecular orbital will result in a decrease of charge in this molecular orbital. This model, then, indicates an increase in the C-O stretching frequency across the series from V to Cu. Looking at Figure 1 it is seen that the frequency of first main infrared band does indeed increase in the series from V to Cu. Thus this simple molecular orbital model gives the correct qualitative shift from one metal to the next in the series.

A close look at the data of Table I reveals that while the high-frequency band interpreted by this model as CO adsorbed on middle sites increases markedly in this series from V to Cu, the main low-frequency band, interpreted as CO on corner sites, does not change position appreciably. To simulate this phenomenon a more complex molecular orbital model is required. In order to show different behavior in different types of sites the model must be large enough to have different sites. The success of simple molecular orbital models in giving the same qualitative effects as more complex calculations and in showing differences in adsorption behavior at different sites<sup>12</sup> suggests trying a molecular orbital model for CO adsorbed on a small cluster of metal atoms.

As a model of the  $\pi$ -electron system for chemisorbed CO, a square array of nine atoms with a two atom molecule adsorbed at either the corner atom or the middle atom is considered. Only one orbital per atom is used, representing a d orbital on each of the metal atoms of the array and a p orbital on each one of the carbon and oxygen atoms. An extended Hückel-type calculation is done in which the molecular orbitals are assumed to be linear combinations of atomic orbitals, and a secular determinantal equation,  $|H_{ij} - ES_{ij}| = 0$ , is solved for the orbital energies and coefficients. The diagonal effective Hamiltonian elements  $H_{ii}$  are taken as valence-state ionization potentials (VSIP). For p orbitals on carbon and oxygen these are 0.392 and 0.584 au, respectively.<sup>17</sup> To correspond to a metal with an atomic number near that of Ni with some promotion of electrons to s and p orbitals, a value of 0.410 au was chosen for the ionization energy from a d orbital. For a metal with an atomic number near that of Cr under the same conditions, a value of 0.300 au was chosen. The off-diagonal elements  $H_{ij}$  were determined from the equation

$$H_{ij} = 0.80S_{ij}(H_{ii} + H_{jj})$$

Since this is a qualitative model with no attempt to reproduce the actual metal geometry and orbital orientation, the values for overlap elements,  $S_{ij}$ , were arbitrarily chosen with nearest neighbor metal-metal overlap elements of 0.30, carbon-metal overlap 0.30, carbon-oxygen overlap 0.35, and other overlap elements falling off with distance.

The numerical results of the orbital calculation are shown in Tables II and III. Only the orbital coefficients

(17) C. J. Ballhausen and H. B. Gray, "Molecular Orbital Theory," W. A. Benjamin, Inc., New York, N. Y., 1965.

**Table II.** Some Molecular Orbital Coefficients Using a Metal VSIP of 0.410 au, Representative of Ni<sup>a</sup>

| Orbital no.           | Energy, au | Carbon coef | Oxygen coef | Metal coef | C-O region         | M-C region         |
|-----------------------|------------|-------------|-------------|------------|--------------------|--------------------|
| CO Attached to Corner |            |             |             |            |                    |                    |
| 1                     | -0.605     | 0.253       | 0.852       | 0.103      | Strongly bonding   | Bonding            |
| 2                     | -0.552     | 0.022       | 0.135       | -0.162     | Nonbonding         | Nonbonding         |
| 3                     | -0.457     | 0.011       | -0.017      | 0.117      | Nonbonding         | Nonbonding         |
| 4                     | -0.455     | 0.089       | -0.228      | 0.423      | Weakly antibonding | Weakly bonding     |
| 5                     | -0.372     | 0.307       | -0.308      | 0.550      | Antibonding        | Bonding            |
| 6                     | -0.356     | 0.181       | -0.132      | 0.120      | Antibonding        | Weakly bonding     |
| 7                     | -0.348     | 0.026       | -0.063      | 0.021      | Nonbonding         | Nonbonding         |
| 8                     | -0.285     | 0.615       | -0.339      | 0.090      | Antibonding        | Weakly bonding     |
| 9                     | -0.254     | 0.024       | -0.057      | 0.115      | Nonbonding         | Nonbonding         |
| 10                    | -0.206     | 0.777       | -0.318      | -0.693     | Antibonding        | Antibonding        |
| 11                    | -0.103     | 0.253       | -0.084      | -0.500     | Antibonding        | Antibonding        |
| CO Attached to Middle |            |             |             |            |                    |                    |
| 1                     | -0.608     | 0.239       | 0.810       | 0.112      | Strongly bonding   | Bonding            |
| 2                     | -0.543     | 0.063       | 0.373       | -0.234     | Weakly bonding     | Weakly antibonding |
| 3                     | -0.457     | 0.000       | 0.000       | 0.000      | Nonbonding         | Nonbonding         |
| 4                     | -0.457     | 0.000       | 0.000       | 0.000      | Nonbonding         | Nonbonding         |
| 5                     | -0.366     | 0.000       | 0.000       | 0.000      | Nonbonding         | Nonbonding         |
| 6                     | -0.361     | 0.363       | -0.312      | 0.742      | Antibonding        | Bonding            |
| 7                     | -0.348     | 0.000       | 0.000       | 0.000      | Nonbonding         | Nonbonding         |
| 8                     | -0.264     | 0.941       | -0.479      | -0.270     | Antibonding        | Antibonding        |
| 9                     | -0.255     | 0.000       | 0.000       | 0.000      | Nonbonding         | Nonbonding         |
| 10                    | -0.255     | 0.000       | 0.000       | 0.000      | Nonbonding         | Nonbonding         |
| 11                    | -0.082     | 0.409       | -0.132      | -0.866     | Antibonding        | Antibonding        |

<sup>a</sup> The metal atom coefficient is for that atom to which the carbon atom is bonded.

**Table III.** Some Molecular Orbital Coefficients Using a Metal VSIP of 0.300 au, Representative of Cr<sup>a</sup>

| Orbital no.           | Energy, au | Carbon coef | Oxygen coef | Metal coef | C-O bond         | M-C bond       |
|-----------------------|------------|-------------|-------------|------------|------------------|----------------|
| CO Attached to Corner |            |             |             |            |                  |                |
| 1                     | -0.603     | 0.258       | 0.876       | 0.018      | Strongly bonding | Weakly bonding |
| 2                     | -0.405     | 0.066       | -0.095      | 0.185      | Nonbonding       | Nonbonding     |
| 3                     | -0.345     | 0.433       | -0.359      | 0.459      | Antibonding      | Bonding        |
| 4                     | -0.334     | 0.004       | -0.008      | -0.069     | Nonbonding       | Nonbonding     |
| 5                     | -0.298     | 0.616       | -0.375      | 0.204      | Antibonding      | Bonding        |
| 6                     | -0.262     | 0.131       | -0.050      | -0.141     | Nonbonding       | Antibonding    |
| 7                     | -0.255     | 0.022       | -0.040      | -0.024     | Nonbonding       | Nonbonding     |
| 8                     | -0.229     | 0.545       | -0.231      | -0.338     | Antibonding      | Antibonding    |
| 9                     | -0.186     | 0.019       | -0.043      | 0.092      | Nonbonding       | Nonbonding     |
| 10                    | -0.163     | 0.507       | -0.175      | -0.789     | Antibonding      | Antibonding    |
| 11                    | -0.076     | 0.192       | -0.059      | -0.492     | Nonbonding       | Antibonding    |
| CO Attached to Middle |            |             |             |            |                  |                |
| 1                     | -0.603     | 0.258       | 0.876       | 0.015      | Strongly bonding | Nonbonding     |
| 2                     | -0.403     | 0.141       | -0.242      | 0.263      | Antibonding      | Bonding        |
| 3                     | -0.335     | 0.000       | 0.000       | 0.000      | Nonbonding       | Nonbonding     |
| 4                     | -0.335     | 0.000       | 0.000       | 0.000      | Nonbonding       | Nonbonding     |
| 5                     | -0.299     | 0.801       | -0.478      | 0.422      | Antibonding      | Bonding        |
| 6                     | -0.268     | 0.000       | 0.000       | 0.000      | Nonbonding       | Nonbonding     |
| 7                     | -0.255     | 0.000       | 0.000       | 0.000      | Nonbonding       | Nonbonding     |
| 8                     | -0.227     | 0.640       | -0.276      | -0.655     | Antibonding      | Antibonding    |
| 9                     | -0.186     | 0.000       | 0.000       | 0.000      | Nonbonding       | Nonbonding     |
| 10                    | -0.186     | 0.000       | 0.000       | 0.000      | Nonbonding       | Nonbonding     |
| 11                    | -0.061     | 0.328       | -0.099      | -0.874     | Antibonding      | Antibonding    |

<sup>a</sup> The metal atom coefficient is for that atom to which the carbon atom is bonded.

for carbon, oxygen, and the metal atom to which the carbon is bonded are given. Coefficients for the other eight metal atoms are available upon request.

Considering first the case where the metal VSIP is taken as 0.410 au, the orbital coefficients follow the same pattern as the previous molecular orbital model using only one metal atom. That is, with one metal atom the lowest energy orbital is bonding for both the C-O and M-C bonds, the next lowest orbital is antibonding for the C-O bond and bonding for the M-C bond, and the highest energy orbital is antibonding for both bonds. For adsorption on the nine-atom array on both the corner and middle sites, it is seen in Table

II that the lowest energy orbital is bonding for the C-O and M-C bonds, that along in the middle energy orbitals numbered 4 to 6 the C-O region is antibonding and the M-C region bonding, and that the high-energy orbitals are antibonding. Nonbonding orbitals are dispersed between these groupings. Thus with partial filling of the orbitals the one metal atom model and the metal cluster model give the same relative bonding and antibonding behavior so that all statements about bond-order changes and related infrared band shifts with addition of other gases, alloying, etc., apply equally well to both models.

For the metal VSIP taken as 0.300 au, Table III

indicates that the same considerations hold with the important change that now the antibonding character in the C-O bond begins occurring in the second and third orbitals. Thus to have a stable adsorbed CO species there must be fewer electrons put into these molecular orbitals. Since this case is for a metal with a lower atomic number than previously, there will be fewer d electrons available for these orbitals. Thus this model does show appropriate and necessary changes in orbitals as the atomic number and number of d electrons are changed across the transition metal series to have a stable adsorbed CO species. This is in agreement with the experimental finding of stable adsorbed CO on this series with CO bond orders, inferred from infrared spectra, that are similar.

Although CO bond orders are similar across the series, the infrared data indicate they do change and that bond orders for CO on the two different sites change by different relative amounts across the series. Bond orders may be calculated from the molecular orbitals as the overlap population defined by Mulliken.<sup>18</sup> This overlap population  $n_{ij}$  for the bonding of atoms  $i$  and  $j$  is defined by

$$n_{ij} = \sum 2N_p S_{ij} C_{ip} C_{jp}$$

where the sum is over the occupied orbitals labeled by  $p$ ,  $N_p$  is the number of electrons in orbital  $p$ , and  $C_{ip}$  and  $C_{jp}$  are the orbital coefficients for atoms  $i$  and  $j$  in orbital  $p$ . Using eight electrons with the Ni representation and 4.4 electrons with the Cr representation, the C-O bond orders are corner Ni, 0.276; middle Ni, 0.304; corner Cr, 0.264; and middle Cr, 0.268. For CO adsorbed on corner sites the C-O bond orders increase only slightly with atomic number, *i.e.*, increasing metal VSIP. The C-O bond orders on the low atomic number metal are close together. For CO adsorbed on middle sites the C-O bond order increases with increasing atomic number. All of these features of the calculated bond orders fit the behavior of the infrared bands shown in Figure 1 when the previously given assumption that the high-frequency band repre-

sents CO adsorbed on middle sites and the lower frequency band adsorption on corner sites is used.

Quantum mechanical calculations for adsorption on idealized semiinfinite model crystals have dwelt on the existence of localized states.<sup>10,11</sup> In a recent paper on molecular orbital calculations for chemisorption on finite idealized crystals it was shown that even where a localized orbital is formed, all occupied orbitals are important in determining bond orders for the adsorption bond.<sup>12</sup> To what extent localized orbitals are formed by real systems is an unanswered question. Previous calculations indicate that the formation of a localized state is largely dependent on the atomic orbital energy of the adsorbate relative to the adsorbent atoms. The use of VSIP's for the diagonal terms in these molecular orbital calculations should place the atoms in approximately the correct energies relative to each other, thereby giving a correct indication of the formation or lack thereof of a localized state. For the  $\pi$ -electron system of chemisorbed CO, these calculations indicate the formation of a localized state. The lowest energy orbital in all cases has only a small atomic orbital coefficient on the metal atom to which the carbon atom is bonded and the metal atom coefficients decrease monotonically as the metal atom becomes further from the adsorbed species. However, not in all cases is the localized orbital the largest contributor to the M-C bond order, and certainly in all cases other orbitals are important in determining M-C and C-O bond orders.

It should be noted that the  $\sigma$ -bonding system has not been considered in this model so that all variations in site and metal are blamed on the  $\pi$  network. This is probably not entirely correct. Also the number of electrons put into the orbitals is chosen to give the desired results. With these ambiguities in mind, the main point is that one can readily explain the data within the framework of a relatively simple molecular orbital model, thereby demonstrating that molecular orbital models which have been so successful in handling ordinary organic and inorganic systems are equally useful in understanding surface species.

**Acknowledgment.** This work was partially supported by a grant from the National Science Foundation.

(18) R. S. Mulliken, *J. Chem. Phys.*, **23**, 1833, 1841, 2338, 2343 (1955).